Int. J. Microgravity Sci. Appl., **37** (4) (2020) 370404
DOI: 10.15011/jasma.37.4.370404

IIII Original Paper IIII

Crystal Structure Analysis of the 20S Proteasome Grown in Space: Comparison between Space and Ground Crystals

Yukio MORIMOTO [1], Masayuki KAMO [2], Naoki FURUBAYASHI [2], Yuuki HIGASHINO [2] and Koji INAKA [2]

Abstract

Microgravity utilization in space is a powerful technique for high-quality protein crystallization. Drug design requires information regarding three-dimensional atomic coordinates from a precious protein structure at atomic resolution. Crystals obtained in space have greater availability for the analysis of drug/protein interactions compared to crystals on the ground. In this study, we assessed the reliabilities of crystal characterization based on the mosaicities of the space and ground crystals and determined a complex whole structure of the 20S proteasome with an anticancer drug.

Keyword(s): Anti-cancer drug, Proteasome, Mosaicity, Inhibitor complex.
Received 27 August 2020, Accepted 13 October 2020, Published 31 October 2020.

1. Introduction

It is important for drug design that high-accuracy three-dimensional protein structures, especially for severe diseases in humans, are determined. At the active site, a mechanism between substrate or inhibitor drugs and amino acid residues of the protein is described as a host-guest reaction with atomic resolution to design or create a new chemical compound. Therefore, many drugs have been developed for use in clinical medicine, such as anticancer drugs[1,2]. Effective drugs are developed using accurate information led by high-resolution drug and protein coordinates. Generally, high accuracy determination requires high-quality protein crystals due to their better signal/noise data. There are some effects on crystallization, purity, concentration, and precipitants. Conditions or environmental factors that we do not pay much attention to on a daily basis (such as temperature, pressure, air, and gravity) can sometimes affect crystallization. To our knowledge, life on earth has always existed alongside gravity[3]. Because the potential energy of a material caused by its mass and gravitational acceleration becomes more dominant than thermal energy according to thermodynamics, in crystallization, a large molecular weight complex might sink in a crystallization capillary due to its weight. The 20S proteasome is composed of 28 subunits and has a molecular weight of 750 kDa[4]. This proteasome is an important enzyme complex in living cells for the maintenance of suitable cell metabolism by the degradation of unneeded proteins. The inhibition of the 20S enzymatic activity suppresses the proliferation of cancer cells, indicating that inhibitors of the 20S proteasome play a role in functioning of anticancer drugs[5]. For analyses of the correct screening and/or docking mechanisms between drugs and enzymes, a complex crystal with suitable resolution is required. Microgravity crystallization[6-8] may be suitable for this purpose.

It is not possible to reduce or completely eliminate the influence of gravity on earth except through a quasi-microgravity method using a magnetic field[9,10], despite technological advancements. It is possible to create a gravity-free condition for an extremely limited amount of time (maximum 5 s) by utilizing free fall. Although the simulated gravity-free conditions are applicable for experiments involving chemical reactions that last a matter of seconds, they are inapplicable for experiments regarding life forms with metabolic turnover that last from several minutes to several hours. Otherwise, a clinostat experiment[11] may disturb a solution in a small vessel when free diffusion is expected. Utilizing the environment in space is a suitable solution for reducing the influence of gravity. The environment in space provides ideal conditions for protein crystallization[12], with reduced convection currents in the solution, resulting in crystals of excellent condition. Drug design, such as anticancer agent development, requires highly accurate structural analysis of protein crystals. In this study, we discuss the crystallization process in the space environment and the analysis of results for improving crystallization quality, which is necessary for the high-precision structural analysis of the 20S proteasome for the development of anticancer drugs.

1 Institute for Integrated Radiation and Nuclear Science, Kyoto University, Kumatori, Osaka 590-0494, Japan.
2 Maruwa Foods and Biosciences Inc., 170-1, Tsutsui-cho, Yamato-koriyama, Nara 639-1123, Japan.
(E-mail: morimoto.yukio.3z@kyoto-u.jp)

 ©2020 The Jpn. Soc. Microgravity Appl.

2. Experiments

2.1 Crystallization of the 20S Proteasome and X-Ray Diffraction Experiment

The 20S proteasome[13] of yeast origin (*Saccharomyces cerevisiae*) was used. The genetically modified yeast strain was subjected to cultivation, fragmentation, and refining to obtain samples for crystallization. Approximately 10 mg of 20S enzyme was harvested from 80 g of yeast[14]. For crystallization, rectangular, planar, transparent crystals were obtained in approximately one week, as shown in **Fig. 1a**, by the counter diffusion (CD)[15,16] method, using 2-methyl-2,4-pentanediol (MPD) as the precipitating agent. The crystals were then cryoprotected by the addition of 40% MPD, and diffraction data collection was performed at 100 K using a macromolecular crystallography beamline BL-44XU from the Institute for Protein Research, Osaka University in the SPring-8 synchrotron radiation facility. Each frame was measured at an oscillation angle of 0.5°/0.5 s of exposure with a 360° total rotation angle, and a total of 720 diffraction images were obtained.

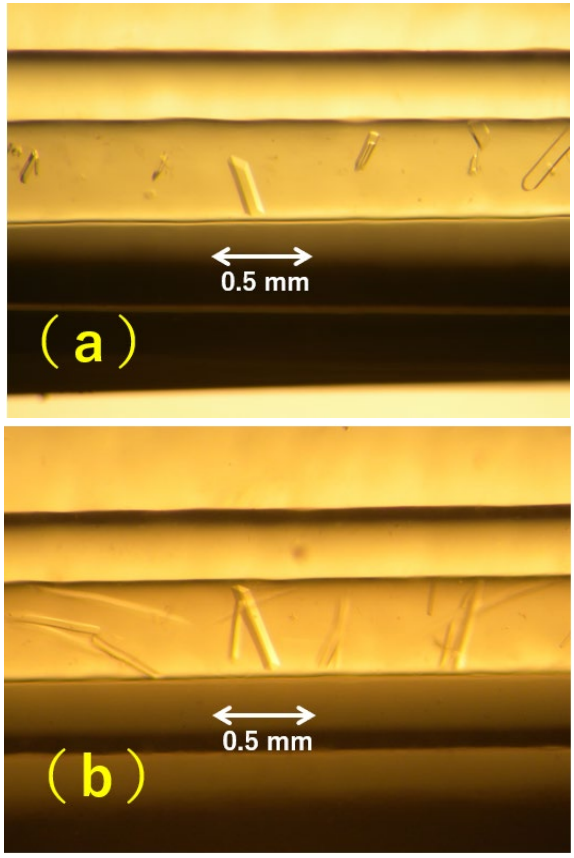

Fig. 1 Microscopic photographs of the 20S proteasome in a glass capillary (a) crystal formed on the ground (control), (b) crystal grown in space in the Japanese experiment module KIBO. Arrows indicate scales.

2.2 Crystallization in the Space Environment

Crystallization of the samples (**Fig. 1b**) was performed inside the hatch of the Japanese Experiment Module (JEM) known as "Japanese Experiment Module KIBO" in the International Space Station, using the CD method, as a part of the low-temperature protein crystal growth experiment (LT PCG, JAXA JEM: High-Quality Protein Crystal Growth Experiment sponsored by the Japan Aerospace Exploration Agency (JAXA))[17], with sample payload launched to orbit by Falcon 9, designed and manufactured by SpaceX, USA. After a crystallization period of approximately four weeks from the initiation of crystallization by the release of the valve between the protein and precipitant reservoir solutions, samples were collected, cryoprotected by the same method as the samples under ground conditions, and subjected to a diffraction experiment at SPring-8 BL-44XU under the same conditions as the crystals on the ground.

3 Results and Discussion

3.1 Crystallization on the Ground and in the Space Environment

Figures 1a and **b** show 20S proteasome crystals formed on the ground and in the space environment, respectively. A glass capillary tube (diameter 1.0 mm) filled with 5 mg/mL protein in 100 mM MES-NaOH, pH 6.5, 20 mM Mg-acetate, 15% MPD, 0.04% NaN_3 was thrust into a precipitation solution with 30% MPD to diffuse back into the protein solution through a partition of agarose gel. The concentrations of protein and types of precipitants in the ground and space crystals were almost identical. A complex form co-crystallized with 10 mM carfilzomib was kept under the same conditions. A vapor diffusion technique is well used in crystallization[18] and allows a gradual increase in the concentration of protein and precipitant in the crystallization solution by vapor equilibrium in the gas-liquid interface. However, single-crystal growth can be prevented by possible Marangoni convection or density difference-induced convection in the space[19] that occurs from the solution surface tension in the protein solution droplets. Therefore, the CD method is usually employed in protein crystallization in the space environment[20], allowing high reproducibility of single-crystal growth without Marangoni convection due to the lack of surface tension, as there is no space between the protein and precipitant solutions and, thus, no gas-liquid concentration diffusion. Moreover, it is possible to increase the precipitant concentration by free diffusion only, without the convection induced by density differences between the protein and precipitant. We confirmed slight differences in the microscopy observations of the crystals obtained by these two crystallizations regarding the size and shape, as shown in **Fig. 1**.

3.2 X-ray Diffraction Experiment

We obtained diffraction data from several crystals without inhibition (i.e., native form) of the ground and space. To select a good quality crystal, we sought factors calculated by a program SCALA/CCP4[21] of R-merge, $CC_{1/2}$, and completeness within the collected data. One of each had diffraction intensities of good quality. **Table 1** shows the results of the X-ray diffraction experiment conducted on crystals formed on the ground (Ground F; F annotated as inhibitor-free) and in the space environment (Space F). The maximum resolution was determined by the visual observation of diffraction images on an Eiger 16M detector and was set through one data collection. The lattice constants and space groups were almost identical in both sets of crystals (**Table 2**). The maximum resolution of each crystal was 2.24 and 1.93 Å, and the efficient reflection range for structural refinement was 2.92 and 2.74 Å, respectively, evidently indicating a higher resolution capability in Space F, which suggests that the molecular packing in the space crystal is stable compared to ground crystal. Additionally, this indicates that the uniformity of crystal formation in the irradiation area where diffraction occurs is higher in particular crystals.

3.3 Crystal Mosaicity

The index of this crystal field uniformity is additionally shown in the parameter obtained from data processing called mosaicity[22]. It is impossible to observe mosaicity using an optical microscope, implying that we cannot evaluate whether a sample is a high-quality crystal with a high-resolution capability from its appearance, as shown in **Fig. 1**.

Figure 2 shows the mosaicity plot obtained from the diffraction measurements in **Table 1** for the Ground F and Space F crystals.

Table 1 Diffraction data statistics of the ground and the space crystals.

Ground F					Space F				
Lower	Upper	R-fac	CC1/2	Compl	Lower	Upper	R-fac	CC1/2	Compl
90.00	6.08	0.042	0.995	0.999	50.00	5.24	0.056	0.992	0.998
6.08	4.83	0.073	0.983	0.996	5.24	4.16	0.082	0.992	0.998
4.83	4.22	0.088	0.976	0.994	4.16	3.63	0.136	0.983	0.996
4.22	3.83	0.109	0.962	0.990	3.63	3.30	0.214	0.962	0.990
3.83	3.56	0.146	0.940	0.984	3.30	3.06	0.377	0.456	0.792
3.56	3.35	0.189	0.900	0.973	3.06	2.88	0.515	0.733	0.920
3.35	3.18	0.239	0.793	0.940	**2.88**	**2.74**	**0.659**	**0.561**	**0.848**
3.18	3.04	0.312	0.622	0.876	2.74	2.62	0.772	0.361	0.728
3.04	**2.92**	**0.354**	**0.485**	**0.808**	2.62	2.52	0.893	0.237	0.619
2.92	2.82	0.389	0.376	0.739	2.52	2.43	0.979	0.153	0.516
2.82	2.73	0.419	0.316	0.693	2.43	2.36	1.023	0.089	0.404
2.73	2.66	0.524	0.201	0.578	2.36	2.29	1.090	0.045	0.292
2.66	2.59	0.450	0.243	0.626	2.29	2.23	1.105	0.007	0.117
2.59	2.52	0.470	0.226	0.607	2.23	2.17	1.156	0.007	0.117
2.52	2.47	0.490	0.201	0.579	2.17	2.12	1.166	0.005	0.099
2.47	2.41	0.499	0.220	0.601	2.12	2.08	1.183	0.007	0.117
2.41	2.36	0.512	0.174	0.544	2.08	2.04	1.187	0.007	0.121
2.36	2.32	0.523	0.177	0.548	2.04	2.00	1.183	0.012	0.155
2.32	2.28	0.550	0.166	0.534	2.00	1.96	1.167	0.001	0.048
2.28	2.24	0.668	0.133	0.485	1.96	1.93	1.156	0.006	0.106

Lower, Upper shows resolution as shell, R-fac is reliability factors of intensity averaging, $CC_{1/2}$ is correlation factor with background correction and Compl is completeness of the data. Underline gives suitable data shell for structural analysis.

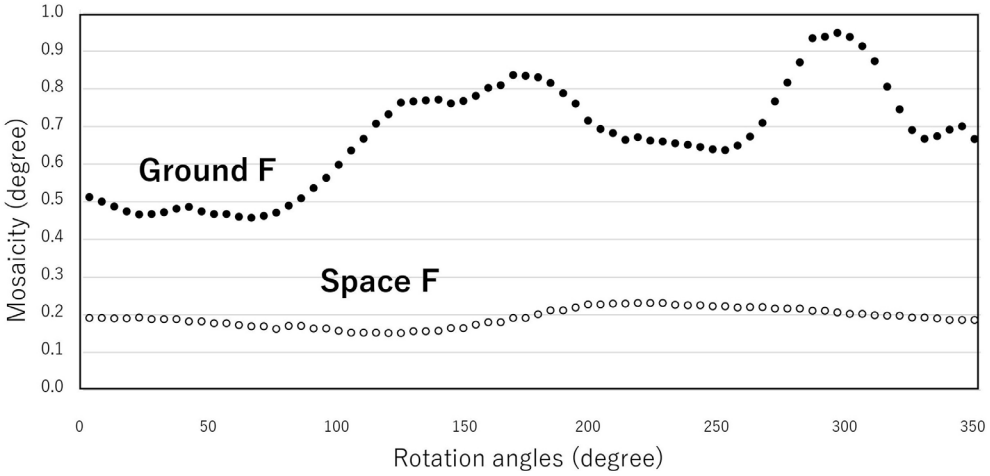

Fig. 2 Plots of mosaicity of ground and space crystals against rotation angle.

Figure 2 shows a low degree of mosaicity in Space F. Compared with Ground F, which shows approximately 0.5–0.9 degrees, Space F shows a degree of only approximately 0.2. Additionally, Ground F shows increases and decreases in mosaicity at the 180° rotation intervals, but Space F does not. This suggests that the mosaicity differences, at least in the two directions crossing the crystal rotation axis, are minimal, showing high isotropy (or crystal uniformity) in the two directions. This suggests that hindrances to crystal growth in the vertical direction are minimal under the microgravity environment.

Mosaicity may lead to a gap or discrepancy of the crystal, causing growth to terminate at a limitation, defining the size of the crystal, making a repetition of uniform area impossible due to the large gap generated at the end of growth.

Space F indicates a low level of mosaicity, suggesting that the terminal point of crystal growth should be relatively distant, resulting in the enhancement of crystal growth with multiple repetitions of the same crystal lattice. Crystal growth under a microgravity environment should thus be an effective method of crystallization with substantial crystal sizes and excellent quality.

3.4 Structural Analysis of the 20S Proteasome

We used reflection data of 2.8 Å resolution for structural analyses and refinements, in which the completeness of data was 73% for Ground F and 85% for Space F. We then determined the overall protein structure through phase determination processes[23,24] from the diffraction data. **Table 2** shows the statistical values of these two crystals and that of the

Table 2 Statistical values of structural refinement.

	Ground F	Space F	Space Carfilzomib
Space group	$P2_1$	$P2_1$	$P2_1$
Cell dimensions (a, b, c (Å), β(°))	135.3, 299.93, 143.77, 112.79	135.04, 300.86, 144.26, 112.82	135.41, 300.67, 143.53, 112.71
Resolution (Å)	150.0 – 2.80	150.20 – 2.80	150.4 – 2.50
No. of reflections	258,532	259,512	363,652
R^a / $R_{free}{}^b$	0.207 / 0.252	0.220 / 0.275	0.223 / 0.272
r.m.s.d. Bond length (Å)	0.008	0.007	0.015
r.m.s.d. Bond angle (°)	1.770	1.595	1.838

[a] $R = \Sigma||F_{obs}|-|F_{calc}||/ \Sigma |F_{obs}|$

[b] R_{work} is calculated from a set of reflections in which 5% of the total reflections have been randomly omitted from the refinement and used to calculate R_{free}.

complex with the anticancer drug carfilzomib. Carfilzomib is an inhibitor of the proteasome that functions as an anticancer drug for myeloma by inducing apoptosis. **Figure 3a** shows the overall protein structure of the 20S proteasome.

This enzyme has a barrel-shaped structure consisting of 14 different types of subunits, with 28 subunits in total. The residues of the catalytic triad of the chymotrypsin-like proteolytic active site contained within the β ring are shown in **Fig. 3c**. The OH group of threonine is essential for activation; however, it is impossible to determine the position of the hydrogen of the OH group with a 2.8 Å resolution capability in this analysis.

On the contrary, several water molecules (H-O-H) exist around the active site (**Fig. 4a**). The figure shows only oxygen atoms (O) in the globe shape (indicated as Wat) instead of H-O-H. Although the active site in Ground F held three water molecules according to the indistinct electron density map, Space F showed a higher quality in the electron density at the same resolution, and we successfully modeled the MPD used as precipitant instead of the water molecule. Such a good quality, traceable, and unbreaking electron density map would be supported by better reflection data of Space F rather than Ground F. For example, the former redundancies of 5–6 are 27.0% at 2.74 Å and 1.3% at 2.73 Å. This may be caused by the low mosaicity of intensities, leading to better reflection data. This suggests that a superior quality electron density map with the use of low mosaicity diffraction data is available for searching drugs and traceable for compound shape by continuous electron density maps.

Water molecules are usually located around the active sites in preparation for substrate reactions, as illustrated in **Fig. 4a**. In this study, we confirmed that MPD in the crystal field replaced these water molecules. In the proteolysis event, the substrate may be introduced to the binding pocket to enhance deprotonation by a threonine hydroxyl group.

Immunoglobulins are excessively expressed in tumor cells, and the 20S proteasome is highly expressed in response to immunoglobulin expression, fully functioning to process and resolve them. Therefore, the following process for the apoptosis of cancer cells is expected: inhibition of this proteolytic reaction that leads to the accumulation of inessential immunoglobulin, which causes metabolic turnover of cancer cells to stop, resulting in the control of cancer cell propagation. This is why a proteasome inhibitor is used as an anticancer drug[25]. A clear and distinguishable electron density map is needed to search and fit the inhibitor on or in the 20S proteasome and to determine how it can bind to the active site. There are several anticancer drugs and inhibitors of the 20S proteasome, including bortezomib, ixazomib, oprozomib, and delanzomib. We used carfilzomib with three aromatic rings and a large molecular weight. **Figure 4c** shows the complex structure of the 20S proteasome with carfilzomib, a specific drug used in the treatment of multiple myeloma. Since the carfilzomib compound has three aromatic rings, the direction and positions of the three aromatic rings require a resolution of at least 2.5 Å, which can separate the aromatic and other alkyl groups. Its resolution capability shows an improved value of 2.5 Å. Additionally, we confirmed that the carfilzomib molecule was situated and bound to Thr1 at the same site where the precipitant MPD is located in **Fig. 4b**. We confirmed the presence of six sites of chymotrypsin-like activities in the overall structure shown in **Fig. 3a**, each of which showed a different form/status of binding.

Furthermore, we obtained crystals of high quality grown under microgravity conditions and prepared them in a complex form with some variations in soaking time, concentration, and incubation with inhibitors. Analyzing the mode or sequence in the binding of the inhibitor should enable the precise analysis of activity inhibition, leading to an improved understanding of the mechanism of action, efficacy, or presence/absence of side effects in the use of anticancer drugs.

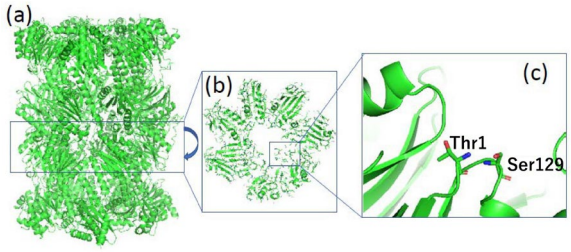

Fig. 3 Diagram of (a) overall structure, (b) β ring, and (c) active site of the 20S proteasome, represented by ribbon drawing of peptide chain with stick model of active Thr1 and Ser129 residues.

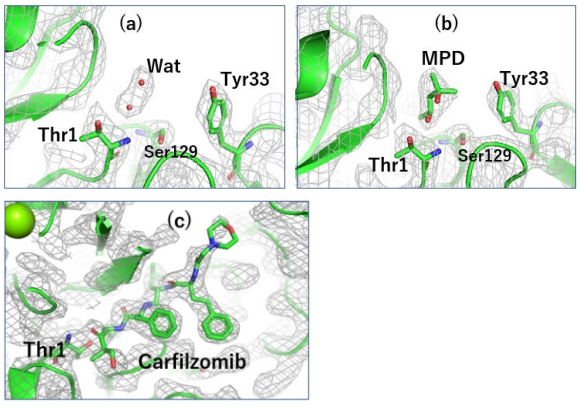

Fig.4 Electron density (2Fo-Fc, 1.5σ) map of chymotrypsin-like active site (H-chain β5 subunit) in the 20S proteasome. (a) water molecules shown in the ground crystal, (b) MPD located instead of water molecules in the space crystal, (c) anti-cancer drug, carfilzomib, bound in the space crystal.

4. Conclusion

In the crystal structure analysis of a large molecular weight enzyme complex, the use of microgravity crystallization is available for precise structure determination. Qualities of crystals grown from ground and space were evaluated from the viewpoint of their crystal mosaicity. The space crystal had relatively low mosaicity, which led to a higher resolution. Crystals under microgravity conditions were efficiently used for enzyme complexes with inhibitors and can clarify the binding chemistry at the active site of the enzyme.

Acknowledgments

This work was partly supported by grants-in-aid from the Terumo Bioscience Foundation 2018 (Y.M.) and the Sumitomo Foundation 2017 (Y.M.). We would like to thank Dr. Kazuya Nishio in the University of Hyogo and Dr. Yasushi Saeki, Prof. Keiji Tanaka in the Tokyo Metropolitan Institute of Medical Science for their helps of proteasome preparation. We also thank the staff members of the JAXA under the proposals 2016-2018JAXPCG#2-6, for their help with the flight of Falcon and Japanese Experiment Module KIBO experiments. Synchrotron radiation experiments were conducted under approvals 2017AB6760, 2018AB6856 and 2019AB6956 of SPring-8 with kind help for X-ray data collection of BL44XU staff.

References

1) H.-S. Cho, K. Mason, K.X. Ramyar, A.M. Stanley, S.B. Gabelli, D.W. Denney Jr. and D.J. Leahy: Nature, **421** (2003) 756.
2) D.L. White, P. Dang, J. Engler, A. Frede, S. Zrim, M. Osborn, V.A. Saunders, P.W. Manley and T.P. Hughes: J. Clin. Oncol., **28** (2010) 2761.
3) S. Furukawa, A. Nagamatsu, M. Nenoi, A. Fujimori, S. Kakinuma, T. Katsube, B. Wang, C. Tsuruoka, T. Shirai, A.J. Nakamura, A. Sakaue-Sawano, A. Miyawaki, H. Harada, M. Kobayashi, J. Kobayashi, T. Kunieda, T. Funayama, M. Suzuki, T. Miyamoto, J. Hidema, Y. Yoshida and A. Takahashi: BioMed. Res. Int., 4703286, (2020).
4) K. Tanaka: Proc. Jpn. Acad. Ser. B Phys. Biol. Sci., **85** (2009) 12.
5) H. Tanaka, K. Inaka, S. Sugiyama, S. Takahashi, S. Sano, M. Sato and S. Yoshitomi: Ann. N. Y. Acad. Sci., **1027** (2004) 10.
6) E.H. Snell, J.R. Helliwell, Rep. Prog. Phys., **68** (2005) 799.
7) A. McPherson, L.J. DeLucas, npj Microgravity, **1** (2015) 15010.
8) S. Takahashi, M. Koga, B. Yan, N. Furubayashi, M. Kamo, K. Inaka and H. Tanaka: Int. J. Microgravity Sci. Appl., **36** (2019) 360107.
9) A. Nakamura, J. Ohtsuka, T. Kashiwagi, N. Numoto, N. Hirota, T. Ode, H. Okada, K. Nagata, M. Kiyohara, E. Suzuki, A. Kita, H. Wada and M. Tanokura: Sci. Rep., **6** (2016) 22127.
10) E.K. Yan, C.Y. Zhang, J. He, and D.C. Yin: Int. J. Mol. Sci., **17** (2016) 1906.
11) Z. Barjaktarović, A. Nordheim, T. Lamkemeyer, C. Fladerer, J. Madlung and R. Hampp: J Exp Bot., **58** (2007) 4357.
12) C.L. Soave, T. Guerin, L. Liu and Q.P. Dou: Cancer Materials Re., **36** (2017) 717.
13) A.P. Arrigo, K. Tanaka and A.L. Goldberg: Nature, **331** (1988) 192.
14) U. Bahrudin, M. Unno, K. Nishio, A. Kita, P. Li, M. Kato, M. Inoue, S. Tsujitani, T. Murakami, R. Sugiyama, Y. Saeki, Y. Obara, K. Tanaka, H. Yamaguchi, I. Sakane, Y Kawata, T. Itoh, H. Ninomiya, I. Hisatome and Y. Morimoto: Sci. Rep. Jul 11, **7** (2017) 5079. doi: 10.1038/s41598-017-04652-2.
15) F. Otálora, J.A. Gavira, J.D. Ng, and J.M. García-Ruiz: Prog. Biophys. Mol. Biol., **101** (2009) 26.
16) Y. Hashizume, K. Inaka, N. Furubayashi, M. Kamo, S. Takahashi and H. Tanaka: Crystals, **10** (2020) 78. doi:10.3390/cryst10020078
17) I. Yoshizaki, M. Yamada, M. Iwata, M. Kato, K. Kihara, T. Ishida, Y. Wada and S. Nagao: Int. J. Microgravity Sci. Appl., **36** (2019) 360101.
18) M. Benvenuti and S. Mangani: Nature Protocol, **2** (2007) 1633.
19) N.E. Chayen and J. Helliwell: Ann. N.Y. Acad. Sci., **974** (2002) 591.
20) H. Tanaka, T. Umehara, K. Inaka, S. Takahashi, R. Shibata, Y. Bessho, M. Sato, S. Sugiyama, E. Fusatomi, T. Terada, M. Shirouzu, S. Sano, M. Motohara, T. Kobayashi, T. Tanaka, A. Tanaka and S. Yokoyama: Acta. Crystallogr., **F63** (2007) 69.
21) P.R. Evans: Acta Crystallogr., **D62** (2006) 72.
22) C.G. Darwin: Phil. Mag., **43** (1922) 800.
23) M. Unno, T. Mizushima, Y. Morimoto, Y. Tomisugi, K. Tanaka, N. Yasuoka, and T. Tsukihara: J. Biol., **131** (2002) 171.
24) M. Unno, T. Mizushima, Y. Morimoto, Y. Tomisugi, K. Tanaka, N. Yasuoka and T. Tsukihara: Structure, **10** (2002) 609.
25) J. Adams ed.: Proteasome Inhibitors in Cancer Therapy, Humana Press (2004).